Robust Iris Segmentation Based on Fully Convolutional Networks and Generative Adversarial Networks

Cides S. Bezerra[1], Rayson Laroca[1], Diego R. Lucio[1], Evair Severo[1], Lucas F. Oliveira[1], Alceu S. Britto Jr.[2] and David Menotti[1]

[1]Federal University of Paraná (UFPR), Curitiba, PR, Brazil
[2]Pontifical Catholic University of Paraná (PUCPR), Curitiba, PR, Brazil

October 31st, 2018

Summary

- Introduction
- Proposed Architecture
- Experiments and Protocols
- Results
- Conclusions and Future Works

Summary

1. Introduction
   - Problem Definition
   - Motivation & Contributions
2. Proposed Architecture
   - Proposed Architecture
3. Experiments and Protocols
   - Experiments and Protocols
4. Results
   - Results
5. Conclusions and Future Works
   - Conclusions and Future Works

UFPR

Visão Robótica Imagem

Problem Definition

- The periocular region as input for the iris biometric system;
  - Iris, pupil, sclera, reflections, eyelids, eyelashes, etc;

Problem Definition

- The periocular region as input for the iris biometric system;
  - Iris, pupil, sclera, reflections, eyelids, eyelashes, etc;
- It is necessary to remove them, as they interfere in the system performance;

Problem Definition

- The periocular region as input for the iris biometric system;
  - Iris, pupil, sclera, reflections, eyelids, eyelashes, etc;
- It is necessary to remove them, as they interfere in the system performance;

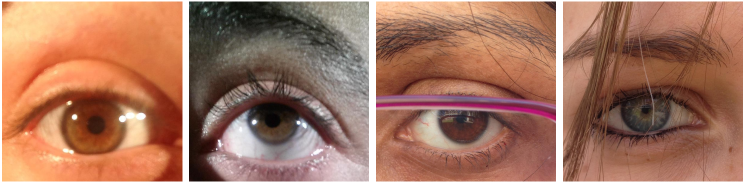

(a) (b) (c) (d)

Figure: Font: (Marsico et al., 2015).

UFPR

Visão Robótica Imagem

Motivation & Contributions

- Convolutional Neural Networks (CNNs) learn representations from training;
- Achieve the state-of-the-art in several computer vision problems;
  - Segmentation, detection, medical images, security systems, etc;
- We propose the use of Fully Convolutional Network (FCN) and Generative Adversarial Networks (GAN);
- More than 2,000 manually labeled images for iris segmentation.

Summary

Architecture FCN - MultiNet (Shelhamer, Long, and Darrell, 2015)

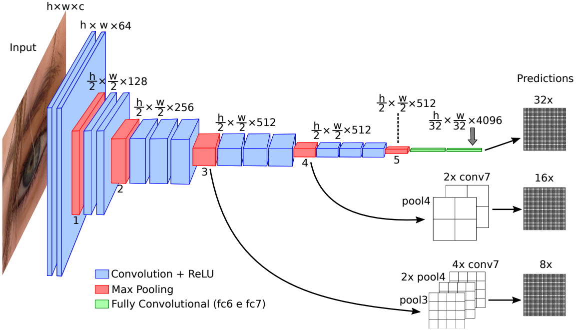

Figure: FCN architecture for iris segmentation. Font: adapted from (Simonyan and Zisserman, 2014).

Architecture GAN - Conditional GAN (Isola et al., 2016)

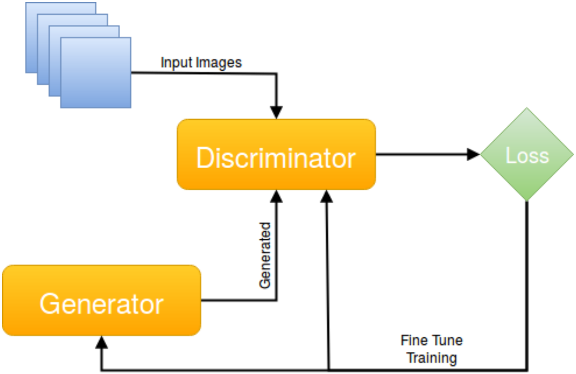

Figure: GAN architecture for iris segmentation.

Preprocessing - Periocular Region Detection

Table: Fast-YOLO network used for iris detection (Severo et al., 2018).

	Layer	Filters	Size	Input	Output
0	conv	16	$3 \times 3/1$	$416 \times 416 \times 1/3$	$416 \times 416 \times 16$
1	max		$2 \times 2/2$	$416 \times 416 \times 16$	$208 \times 208 \times 16$
2	conv	32	$3 \times 3/1$	$208 \times 208 \times 16$	$208 \times 208 \times 32$
3	max		$2 \times 2/2$	$208 \times 208 \times 32$	$104 \times 104 \times 32$
4	conv	64	$3 \times 3/1$	$104 \times 104 \times 32$	$104 \times 104 \times 64$
5	max		$2 \times 2/2$	$104 \times 104 \times 64$	$52 \times 52 \times 64$
6	conv	128	$3 \times 3/1$	$52 \times 52 \times 64$	$52 \times 52 \times 128$
7	max		$2 \times 2/2$	$52 \times 52 \times 128$	$26 \times 26 \times 128$
8	conv	256	$3 \times 3/1$	$26 \times 26 \times 128$	$26 \times 26 \times 256$
9	max		$2 \times 2/2$	$26 \times 26 \times 256$	$13 \times 13 \times 256$
10	conv	512	$3 \times 3/1$	$13 \times 13 \times 256$	$13 \times 13 \times 512$
11	max		$2 \times 2/1$	$13 \times 13 \times 512$	$13 \times 13 \times 512$
12	conv	1024	$3 \times 3/1$	$13 \times 13 \times 512$	$13 \times 13 \times 1024$
13	conv	1024	$3 \times 3/1$	$13 \times 13 \times 1024$	$13 \times 13 \times 1024$
14	conv	30	$1 \times 1/1$	$13 \times 13 \times 1024$	$13 \times 13 \times 30$
15	detection				

UFPR

Visão Robótica Imagem

Architecture - Details

- The detected iris input image is padded/expanded to a power of 2;
- FCN - no fully connected layers, losses spatial information
- GAN - able to capture the statistical distribution of training data

Summary

UFPR

Visão Robótica Imagem

Datasets

Table: Overview of the iris datasets used in this work, where (*) means that only part of the dataset was used.

Dataset	Images	Subjects	Resolution	Wavelength
BioSec (*)	400	25	640×480	NIR
CasiaI3	2,639	249	320×280	NIR
CasiaT4 (*)	1,000	50	640×480	NIR
IITD-1	2,240	224	320×240	NIR
NICE.I	945	n/a	400×300	VIS
CrEye-Iris (*)	1,000	120	400×300	VIS
MICHE-I (*)	1,000	75	Various	VIS

Protocols

- 3 Benchmarks/baselines:
  - OSIRISv4.1 - Open Source Iris ...
  - IRISSEG - Iris Seg Master (in the literature)
  - Haindl & Krupička (Haindl and Krupička, 2015);

Protocols

- 3 Benchmarks/baselines:
  - OSIRISv4.1 - Open Source Iris ...
  - IRISSEG - Iris Seg Master (in the literature)
  - Haindl & Krupička (Haindl and Krupička, 2015);
- 80% train and 20% test;

Protocols

- 3 Benchmarks/baselines:
  - OSIRISv4.1 - Open Source Iris ...
  - IRISSEG - Iris Seg Master (in the literature)
  - Haindl & Krupička (Haindl and Krupička, 2015);
- 80% train and 20% test;
- Train and test on each specific dataset;

Protocols

- 3 Benchmarks/baselines:
  - OSIRISv4.1 - Open Source Iris ...
  - IRISSEG - Iris Seg Master (in the literature)
  - Haindl & Krupička (Haindl and Krupička, 2015);
- 80% train and 20% test;
- Train and test on each specific dataset;
- Merge datasets in the NIR spectrum;

Protocols

- 3 Benchmarks/baselines:
  - OSIRISv4.1 - Open Source Iris ...
  - IRISSEG - Iris Seg Master (in the literature)
  - Haindl & Krupička (Haindl and Krupička, 2015);
- 80% train and 20% test;
- Train and test on each specific dataset;
- Merge datasets in the NIR spectrum;
- Merge datasets in the VIS spectrum;

Protocols

- 3 Benchmarks/baselines:
  - OSIRISv4.1 - Open Source Iris ...
  - IRISSEG - Iris Seg Master (in the literature)
  - Haindl & Krupička (Haindl and Krupička, 2015);
- 80% train and 20% test;
- Train and test on each specific dataset;
- Merge datasets in the NIR spectrum;
- Merge datasets in the VIS spectrum;
- Merge all datasets (both NIR and VIS);

Protocols

- 3 Benchmarks/baselines:
  - OSIRISv4.1 - Open Source Iris ...
  - IRISSEG - Iris Seg Master (in the literature)
  - Haindl & Krupička (Haindl and Krupička, 2015);
- 80% train and 20% test;
- Train and test on each specific dataset;
- Merge datasets in the NIR spectrum;
- Merge datasets in the VIS spectrum;
- Merge all datasets (both NIR and VIS);
- 5-folds;

Protocols

- 3 Benchmarks/baselines:
  - OSIRISv4.1 - Open Source Iris ...
  - IRISSEG - Iris Seg Master (in the literature)
  - Haindl & Krupička (Haindl and Krupička, 2015);
- 80% train and 20% test;
- Train and test on each specific dataset;
- Merge datasets in the NIR spectrum;
- Merge datasets in the VIS spectrum;
- Merge all datasets (both NIR and VIS);
- 5-folds;
- 32,000 iterations.

Summary

Results NICE.I contest.

Table: Iris segmentation results using the NICE.I contest protocol.

Dataset	Method	F1 %	*E* %
NICE.I (VIS)	OSIRISv4.1	30.70 ± 32.00	08.67 ± 06.29
	IRISSEG	21.76 ± 32.13	14.03 ± 12.33
	Haindl & Krupička	75.54 ± 22.93	03.27 ± 04.29
	FCN Proposed	$\mathbf{88.20 \pm 13.73}$	$\mathbf{01.05 \pm 00.86}$
	GAN Proposed	$\mathbf{91.42 \pm 03.81}$	$\mathbf{03.09 \pm 01.76}$

Our protocol

Table: Iris segmentation results using the proposed protocol.

Dataset	Method	F1 %	*E* %
BioSec (NIR)	OSIRISv4.1	92.62 ± 03.19	01.21 ± 00.47
	IRISSEG	93.94 ± 05.88	01.06 ± 01.20
	FCN Proposed	$\mathbf{97.46 \pm 00.74}$	$\mathbf{00.44 \pm 00.12}$
	GAN Proposed	$\mathbf{96.82 \pm 02.83}$	$\mathbf{00.74 \pm 01.40}$

Our protocol

Table: Iris segmentation results using the proposed protocol.

Dataset	Method	F1 %	*E* %
BioSec (NIR)	OSIRISv4.1	92.62 ± 03.19	01.21 ± 00.47
	IRISSEG	93.94 ± 05.88	01.06 ± 01.20
	FCN Proposed	$\mathbf{97.46 \pm 00.74}$	$\mathbf{00.44 \pm 00.12}$
	GAN Proposed	$\mathbf{96.82 \pm 02.83}$	$\mathbf{00.74 \pm 01.40}$
CasiaI3 (NIR)	OSIRISv4.1	89.49 ± 05.78	05.35 ± 02.40
	IRISSEG	94.61 ± 03.28	02.85 ± 01.62
	FCN Proposed	$\mathbf{97.90 \pm 00.68}$	$\mathbf{01.15 \pm 00.37}$
	GAN Proposed	$\mathbf{96.13 \pm 05.35}$	$\mathbf{01.45 \pm 03.71}$

Our protocol

Table: Iris segmentation results using the proposed protocol.

Dataset	Method	F1 %	*E* %
BioSec (NIR)	OSIRISv4.1	92.62 ± 03.19	01.21 ± 00.47
	IRISSEG	93.94 ± 05.88	01.06 ± 01.20
	FCN Proposed	**97.46 ± 00.74**	**00.44 ± 00.12**
	GAN Proposed	**96.82 ± 02.83**	**00.74 ± 01.40**
CasiaI3 (NIR)	OSIRISv4.1	89.49 ± 05.78	05.35 ± 02.40
	IRISSEG	94.61 ± 03.28	02.85 ± 01.62
	FCN Proposed	**97.90 ± 00.68**	**01.15 ± 00.37**
	GAN Proposed	**96.13 ± 05.35**	**01.45 ± 03.71**
CasiaT4 (NIR)	OSIRISv4.1	87.76 ± 08.01	01.34 ± 00.64
	IRISSEG	91.39 ± 08.13	00.95 ± 00.54
	FCN Proposed	**94.42 ± 07.54**	**00.61 ± 00.58**
	GAN Proposed	**95.38 ± 03.72**	**01.40 ± 00.93**

Our protocol

Table: Iris segmentation results using the proposed protocol.

Dataset	Method	F1 %	*E* %
BioSec (NIR)	OSIRISv4.1	92.62 ± 03.19	01.21 ± 00.47
	IRISSEG	93.94 ± 05.88	01.06 ± 01.20
	FCN Proposed	**97.46 ± 00.74**	**00.44 ± 00.12**
	GAN Proposed	**96.82 ± 02.83**	**00.74 ± 01.40**
CasiaI3 (NIR)	OSIRISv4.1	89.49 ± 05.78	05.35 ± 02.40
	IRISSEG	94.61 ± 03.28	02.85 ± 01.62
	FCN Proposed	**97.90 ± 00.68**	**01.15 ± 00.37**
	GAN Proposed	**96.13 ± 05.35**	**01.45 ± 03.71**
CasiaT4 (NIR)	OSIRISv4.1	87.76 ± 08.01	01.34 ± 00.64
	IRISSEG	91.39 ± 08.13	00.95 ± 00.54
	FCN Proposed	**94.42 ± 07.54**	**00.61 ± 00.58**
	GAN Proposed	**95.38 ± 03.72**	**01.40 ± 00.93**
IITD-1 (NIR)	OSIRISv4.1	92.20 ± 06.07	04.37 ± 02.69
	IRISSEG	94.25 ± 03.89	03.39 ± 02.16
	FCN Proposed	**97.44 ± 01.78**	**01.48 ± 01.01**
	GAN Proposed	**95.84 ± 04.13**	**01.33 ± 02.65**

UFPR

Visão Robótica Imagem

Results VIS datasets

Table: Iris segmentation results using the proposed protocol.

Dataset	Method	F1 %	*E* %
NICE.I (VIS)	OSIRISv4.1	38.15 ± 33.61	07.92 ± 06.20
	IRISSEG	28.64 ± 35.14	13.48 ± 12.36
	Haindl & Krupička	70.59 ± 26.11	04.72 ± 05.87
	FCN Proposed	$\mathbf{89.54 \pm 13.79}$	$\mathbf{01.00 \pm 00.70}$
	GAN Proposed	$\mathbf{91.12 \pm 05.08}$	$\mathbf{03.34 \pm 02.31}$

Results VIS datasets

Table: Iris segmentation results using the proposed protocol.

Dataset	Method	F1 %	*E* %
NICE.I (VIS)	OSIRISv4.1	38.15 ± 33.61	07.92 ± 06.20
	IRISSEG	28.64 ± 35.14	13.48 ± 12.36
	Haindl & Krupička	70.59 ± 26.11	04.72 ± 05.87
	FCN Proposed	$\mathbf{89.54 \pm 13.79}$	$\mathbf{01.00 \pm 00.70}$
	GAN Proposed	$\mathbf{91.12 \pm 05.08}$	$\mathbf{03.34 \pm 02.31}$
CrEye-Iris (VIS)	OSIRISv4.1	46.53 ± 29.25	13.22 ± 06.33
	IRISSEG	61.72 ± 33.55	10.58 ± 10.38
	Haindl & Krupička	76.81 ± 23.73	05.69 ± 04.58
	FCN Proposed	$\mathbf{97.04 \pm 01.21}$	$\mathbf{00.96 \pm 00.36}$
	GAN Proposed	$\mathbf{92.61 \pm 05.86}$	$\mathbf{03.02 \pm 03.22}$

Results VIS datasets

Table: Iris segmentation results using the proposed protocol.

Dataset	Method	F1 %	*E* %
NICE.I (VIS)	OSIRISv4.1	38.15 ± 33.61	07.92 ± 06.20
	IRISSEG	28.64 ± 35.14	13.48 ± 12.36
	Haindl & Krupička	70.59 ± 26.11	04.72 ± 05.87
	FCN Proposed	**89.54 ± 13.79**	**01.00 ± 00.70**
	GAN Proposed	**91.12 ± 05.08**	**03.34 ± 02.31**
CrEye-Iris (VIS)	OSIRISv4.1	46.53 ± 29.25	13.22 ± 06.33
	IRISSEG	61.72 ± 33.55	10.58 ± 10.38
	Haindl & Krupička	76.81 ± 23.73	05.69 ± 04.58
	FCN Proposed	**97.04 ± 01.21**	**00.96 ± 00.36**
	GAN Proposed	**92.61 ± 05.86**	**03.02 ± 03.22**
MICHE-I (VIS)	OSIRISv4.1	33.85 ± 35.86	01.99 ± 02.90
	IRISSEG	19.34 ± 33.03	01.90 ± 03.37
	Haindl & Krupička	63.12 ± 33.30	01.32 ± 02.10
	FCN Proposed	**83.01 ± 19.47**	**00.37 ± 00.43**
	GAN Proposed	**87.42 ± 13.08**	**03.27 ± 03.13**

UFPR

Visão Robótica Imagem

Suitability NIR training

Table: Suitability (bold lines) for NIR environments.

Dataset	Method	F1 %	*E* %
BioSec	FCN	97.24 ± 00.81	00.58 ± 00.30
	GAN	90.19 ± 05.52	02.22 ± 01.39
CasiaI3	FCN	97.43 ± 00.74	00.55 ± 00.29
	GAN	97.10 ± 01.83	00.75 ± 01.10
CasiaT4	FCN	95.87 ± 02.66	01.25 ± 00.67
	GAN	82.65 ± 13.98	05.52 ± 04.15
IITD-1	FCN	96.47 ± 01.56	00.72 ± 00.59
	GAN	96.18 ± 02.52	01.09 ± 01.80
NIR	**FCN**	$\mathbf{96.69 \pm 01.43}$	$\mathbf{00.78 \pm 00.63}$
	GAN	$\mathbf{94.04 \pm 07.93}$	$\mathbf{01.72 \pm 02.69}$

Suitability VIS training

Table: Suitability (bold lines) for VIS environments.

Dataset	Method	F1 %	*E* %
NICE.I	FCN	90.68 ± 14.01	02.67 ± 02.04
	GAN	91.40 ± 05.18	01.22 ± 00.71
CrEye-Iris	FCN	96.71 ± 01.11	01.12 ± 00.80
	GAN	93.21 ± 02.30	01.88 ± 00.53
MICHE-I	FCN	88.36 ± 11.88	01.90 ± 02.20
	GAN	89.49 ± 06.76	03.11 ± 02.24
VIS	**FCN**	**89.56 ± 12.36**	**02.40 ± 02.21**
	GAN	**92.58 ± 04.89**	**02.80 ± 02.05**

UFPR

Visão Robótica Imagem

Robustness of the iris segmentation approaches

Table: Robustness (bold lines) of the iris segmentation approaches.

Dataset	Method	F1 %	*E* %
BioSec	FCN	96.57 ± 01.14	00.70 ± 00.24
	GAN	85.48 ± 07.63	03.45 ± 01.97
CasiaI3	FCN	97.69 ± 00.82	00.50 ± 00.33
	GAN	93.33 ± 01.98	00.87 ± 00.92
CasiaT4	FCN	95.39 ± 03.20	01.46 ± 01.12
	GAN	85.68 ± 12.92	03.98 ± 02.80
IITD-1	FCN	97.11 ± 01.70	00.61 ± 00.67
	GAN	94.99 ± 03.88	01.28 ± 01.73
NIR	FCN	$96.89 \pm 06,60$	00.82 ± 00.59
	GAN	89.87 ± 07.93	02.39 ± 01.78

UFPR

Visão Robótica Imagem

Robustness of the iris segmentation approaches

Dataset	Method	F1 %	*E* %
NICE.I	FCN	89.25 ± 14.06	03.31 ± 02.77
	GAN	65.56 ± 23.32	11.53 ± 05.87
CrEye-Iris	FCN	96.15 ± 01.90	01.38 ± 01.16
	GAN	88.96 ± 08.98	04.57 ± 04.63
MICHE-I	FCN	80.49 ± 20.65	02.73 ± 02.76
	GAN	61.93 ± 24.97	10.95 ± 06.22
VIS	FCN	88.63 ± 09.15	02.47 ± 02.23
	GAN	72.15 ± 19.03	09.01 ± 05.54
All	**FCN**	**94.36 ± 09.90**	**01.26 ± 01.73**
	GAN	**86.62 ± 17.71**	**04.03 ± 05.28**

Table: Robustness (bold lines) of the iris segmentation approaches.

Qualitative Results NIR datasets

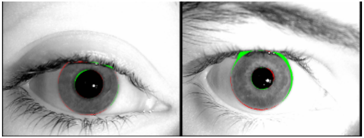

(a) BioSec: FCN 00.31% — 00.85%

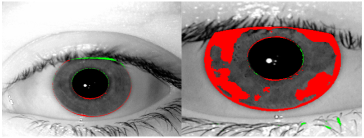

(b) BioSec: GAN 00.27% — 12.61%

Qualitative Results NIR datasets

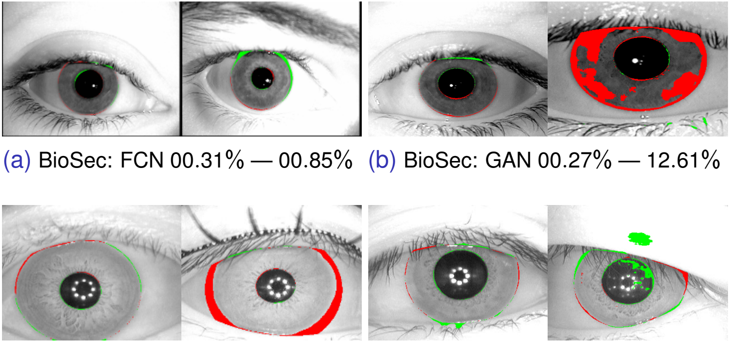

(a) BioSec: FCN 00.31% — 00.85% (b) BioSec: GAN 00.27% — 12.61%

(c) CasiaI3: FCN 00.91% — 05.93% (d) CasiaI3: GAN 00.43% — 01.51%

Figure: FCN and GAN qualitative results: good (left) and bad (right) results based on the error E. Green and red pixels represent the FP and FN, respectively.

UFPR

Visão Robótica Imagem

Qualitative Results NIR datasets

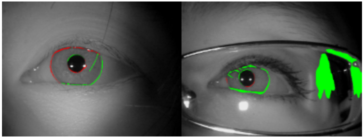

(a) CasiaT4: FCN 00.52% — 04.57%

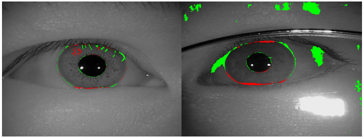

(b) CasiaT4: GAN 00.84% — 06.30%

Qualitative Results NIR datasets

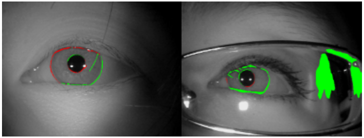

(a) CasiaT4: FCN 00.52% — 04.57%

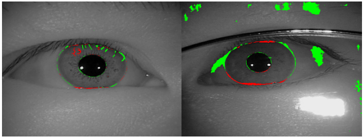

(b) CasiaT4: GAN 00.84% — 06.30%

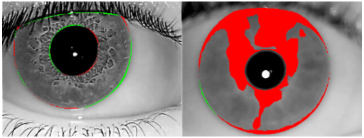

(c) IITD-1: FCN 01.17% — 19.37%

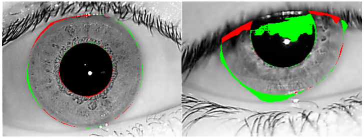

(d) IITD-1: GAN 00.56% — 06.60%

Figure: FCN and GAN qualitative results: good (left) and bad (right) results based on the error *E*. Green and red pixels represent the FP and FN, respectively.

Qualitative Results VIS datasets

(a) NICE.I: FCN 00.95% — 08.28%

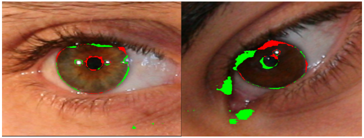

(b) NICE.I: GAN 01.27% — 02.43%

Qualitative Results VIS datasets

(a) NICE.I: FCN 00.95% — 08.28%

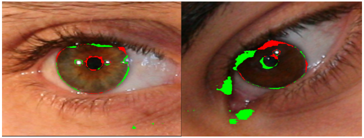

(b) NICE.I: GAN 01.27% — 02.43%

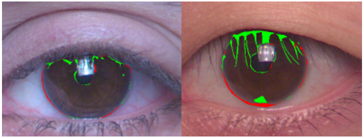

(c) CrEye-Iris: FCN 00.74% — 02.88%

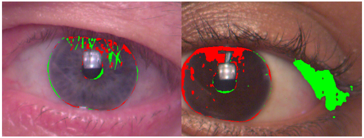

(d) CrEye-Iris: GAN 00.72% — 03.61%

Figure: FCN and GAN qualitative results: good (left) and bad (right) results based on the error *E*. Green and red pixels represent the FP and FN, respectively.

UFPR

Visão Robótica Imagem

Qualitative Results VIS datasets

(a) MICHE-I: FCN 00.42% — 01.82% (b) MICHE-I: GAN 00.57% — 00.96%

Figure: FCN and GAN qualitative results: good (left) and bad (right) results based on the error E. Green and red pixels represent the FP and FN, respectively.

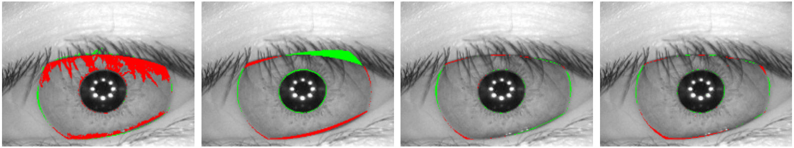

OSIRISv4.1 IrisSeg FCN GAN

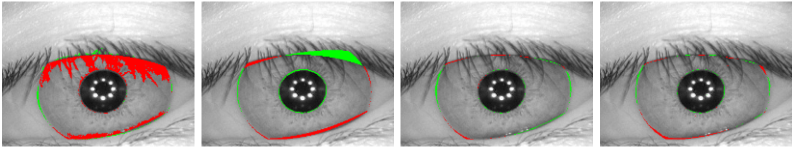

OSIRISv4.1 | IrisSeg | FCN | GAN

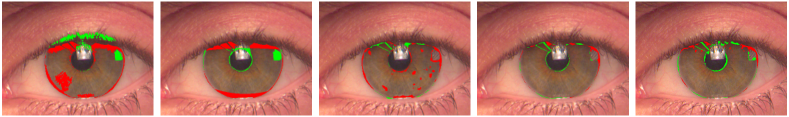

OSIRISv4.1 | IrisSeg | Haindl & Krupička | FCN | GAN

Figure: Qualitative results achieved by the FCN, GAN and baselines. Green and red pixels represent the FP and FN, respectively. The first and second rows correspond, respectively, to CasiaI3 and CrEye-Iris datasets.

Summary

Conclusions

- Two approaches (FCN and GAN) for robust iris segmentation;

Conclusions

- Two approaches (FCN and GAN) for robust iris segmentation;
- Compared with three baselines methods;

Conclusions

- Two approaches (FCN and GAN) for robust iris segmentation;
- Compared with three baselines methods;
- The transfer learning for each domain was essential to achieve outstanding results;

UFPR

Visão Robótica Imagem

Conclusions

- Two approaches (FCN and GAN) for robust iris segmentation;
- Compared with three baselines methods;
- The transfer learning for each domain was essential to achieve outstanding results;
- Pre-trained models from other datasets brings excellent benefits in learning deep networks;

Conclusions

- Two approaches (FCN and GAN) for robust iris segmentation;
- Compared with three baselines methods;
- The transfer learning for each domain was essential to achieve outstanding results;
- Pre-trained models from other datasets brings excellent benefits in learning deep networks;
- We labeled more than 2,000 images for iris segmentation (`https://web.inf.ufpr.br/vri/databases/iris-segmentation-annotations/`).

Future Works

- As future work we intend to:
  - Evaluate the impact of performing the segmentation in two steps (first detection);

Future Works

- As future work we intend to:
  - Evaluate the impact of performing the segmentation in two steps (first detection);
  - Create a post-processing stage to refine the prediction;

Future Works

- As future work we intend to:
  - Evaluate the impact of performing the segmentation in two steps (first detection);
  - Create a post-processing stage to refine the prediction;
  - Classify the sensor or image type and then segment each image with a specific model;

References I

Haindl, M. and M. Krupička (2015). "Unsupervised detection of non-iris occlusions". In: *Pattern Recognition Letters* 57, pp. 60–65. ISSN: 0167-8655. DOI: http://dx.doi.org/10.1016/j.patrec.2015.02.012.

Isola, Phillip et al. (2016). "Image-to-Image Translation with Conditional Adversarial Networks". In: *CoRR* abs/1611.07004. URL: http://arxiv.org/abs/1611.07004.

Marsico, M. et al. (2015). "Mobile Iris Challenge Evaluation (MICHE)-I, biometric iris dataset and protocols". In: *Pattern Recognition Letters* 57, pp. 17–23.

Severo, Evair et al. (2018). "A Benchmark for Iris Location and a Deep Learning Detector Evaluation". In: *2018 International Joint Conference on Neural Networks (IJCNN)*, pp. 1–7. DOI: 10.1109/IJCNN.2018.8489638.

References II

Shelhamer, E., J. Long, and T. Darrell (2015). "Fully Convolutional Networks for Semantic Segmentation". In: *IEEE Transactions on Pattern Analysis and Machine Intelligence* 39.4, pp. 640–651. ISSN: 0162-8828.

Simonyan, K. and A. Zisserman (2014). "Very Deep Convolutional Networks for Large-Scale Image Recognition". In: *CoRR* abs/1409.1556.